Electronic Supplementary Material

Air cathode of zinc-air batteries: a highly efficient and durable aerogel catalyst for oxygen reduction

Lijie Zhang,[a] Xianfeng Yang,[b] Rongsheng Cai[a], Chengmeng Chen[c], Yanzhi Xia[a], Huawei Zhang,[d] Dongjiang Yang*[ae] and Xiangdong Yao*[e]

Experimental Section

ORR: For the electrochemical test, 2 mg of the catalyst was dispersed in the mixture of 50 μL of Nafion (5 wt%) solution, 500 μL of ethanol, and 500 μL distilled water. Then a homogenous catalyst ink was obtained by an ultrasonic disperse method. 6 μL of the ink was pipetted onto a glassy carbon disk (0.0706 cm^{-2}). Measurements were performed in a three-electrode equipped with a Pt counter electrode and a Ag/AgCl reference electrode. Cyclic voltammetry (CV) experiments with a sweep rate of 50 mv s^{-1} were recorded in the potential range of 0 to −1.0 V vs. Ag/AgCl. Linear sweep voltammetry (LSV) was performed in N_2-saturated or O_2-saturated 0.1 M KOH. Current-voltage curves were recorded at a scan rate of 10 mv s^{-1} under various electrode rotation rates (225, 400, 625, 900, 1225, 1600, 2025, and 2500 rpm, respectively). The current density was normalized to the geometrical area and the measured potentials vs. Ag/AgCl were converted to a reversible hydrogen electrode (RHE) scale according to the following equation:

$$E_{\mathrm{RHE}} = E_{\mathrm{Ag/AgCl}} + 0.059 * \mathrm{pH} + 0.1976$$

The electron transfer number (n) of the sample was calculated from the ring current (I_R) and disk current (I_D) through the equation:

$$n = \frac{4NI_D}{NI_D + I_R}$$

The peroxide percentage (H_2O_2%) was calculated based on the equation:

$$H_2O_2 = \frac{200I_R}{NI_D + I_R}$$

Where N = 0.43, N is the current collection efficiency of the Pt ring.

Zinc-air batteries: For a primary zinc-air battery, the air electrode was prepared by uniformly coating the as-prepared catalyst ink onto carbon paper and then drying it at 80 °C for 2 h. The mass loading was 1.25 mg cm^{-2} (0.25 mg cm^{-2} for 20% Pt/C). A zinc plate was used as the anode. Both electrodes were assembled into a home-built electrochemical battery with the electrolyte being 6 M KOH. Polarization data (V-*i*) were collected using linear sweep voltammetry at a scan rate of 10 mV s^{-1}.

The specific capacity normalized to the mass of consumed Zn was calculated based on the equation:

$$\text{The specific capacity} = \frac{\text{current} * \text{serve hours}}{\text{weight of consumed zinc}}$$

The gravimetric energy density normalized to the mass of consumed Zn was calculated based on the equation:

$$\text{The gravimetric energy density} = \frac{\text{current drain} * \text{serve hours} * \text{average discharge voltage}}{\text{weight of consumed zinc}}$$

The power densities of Zn-air batteries were calculated based on the equation: $P=U*j$ (*P* is power densities of zinc-air batteries (mW cm^{-2}), *U* is the battery voltages (V), and *j* is the current densities of batteries (mA cm^{-2})).

DFT Calculations

The density functional theory (DFT) calculations were carried out using the Vienna ab Initio Simulation package (VASP).[1, 2] The ion–electron interactions were described by the projector plane wave（PAW）approach. Electron exchange–correlations were represented by the functional of Perdew, Burke and Ernzerhof (PBE) of generalized gradient approximation (GGA).[3] To ensure the convergence for total energy, all calculations were performed using a plane-wave cutoff energy of 400eV with Fermi-level smearing of 0.1eV and Monkhorst-Pack grid (3×2×2) was used for k-point sampling. Besides, the convergence threshold of energy and forces were set to be 1×10^{-5} eV and 0.02 eV/Å, respectively. The adsorption energy (E_{ads}) of ORR intermediates on catalysts are calculated as

$$E_{ads(\text{intermediate})} = E_{(\text{intermediate/catalyst})} - (E_{\text{catalyst}} + E_{\text{intermediate}})$$

where $E_{(\text{intermediate/catalyst})}$ and E_{catalyst} are the total energies for the optimized equilibrium configurations of catalyst with or without intermediate, respectively, and $E_{\text{intermediate}}$ is the energy of the intermediate in its ground state. Based on these definitions, the negative E_{ads} values correspond to the exothermic stably adsorption processes.

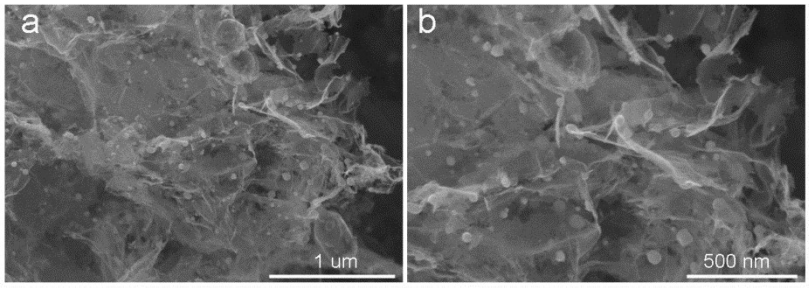

Figure S1. (a) SEM image of the as-synthesized Co_3O_4@Co/N-r-GO and (b) its amplified SEM image.

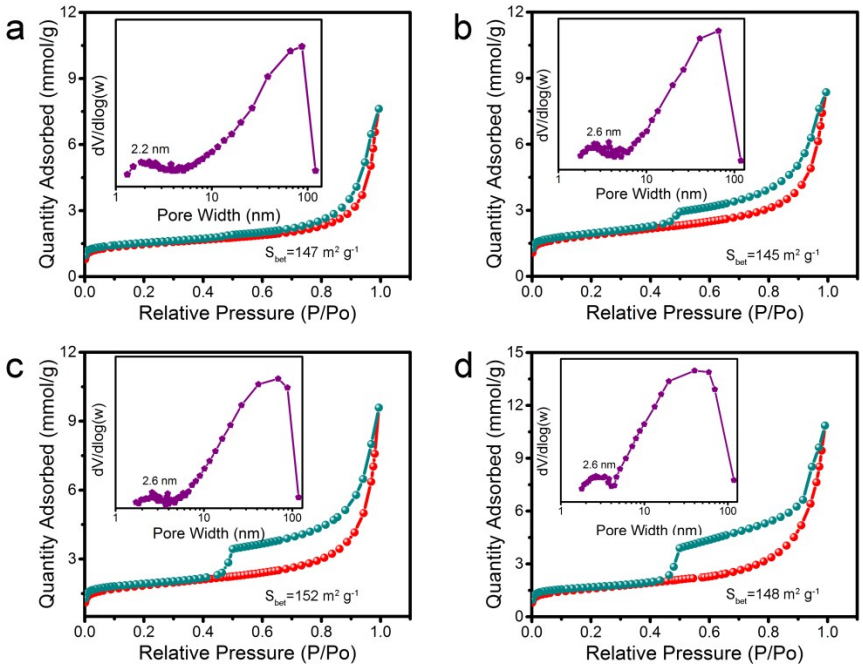

Figure S2. Nitrogen adsorption-desorption isotherms of Co_3O_4@Co/N-r-GO-4 (a), Co_3O_4@Co/N-r-GO-7 (b), Co_3O_4@Co/N-r-GO-15 (c) and Co_3O_4@Co/N-r-GO-20 (d) and their corresponding the pore size distributions (the inset in a, b, c, and d, respectively).

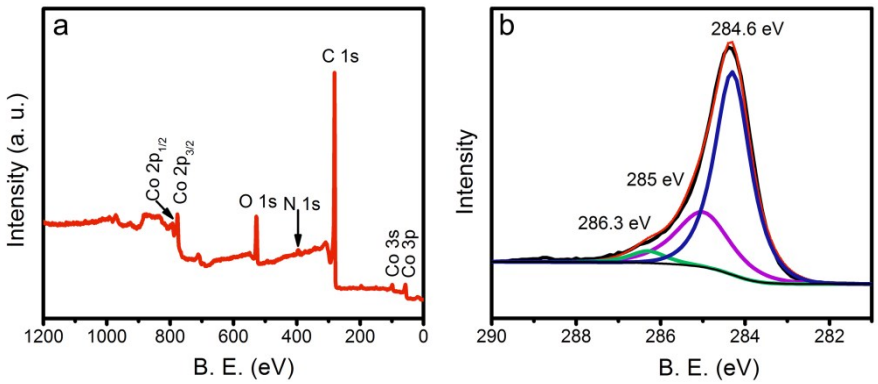

Figure S3. XPS survey and high-resolution XPS spectra for the as-synthesized Co_3O_4@Co/N-r-GO-10.

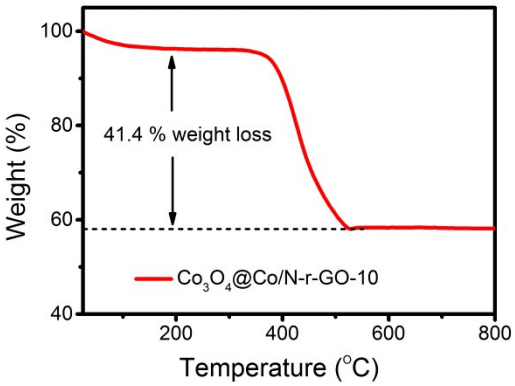

Figure S4. TGA weight change curves of Co_3O_4@Co/N-r-GO-10 tested in air with a ramp rate of 10 °C/min.

As shown in Fig S4, the weight retention is 58.6%. That is to say, after being decomposed at 800 °C in air, 1 g sample contains 0.586 g Co_3O_4, which includes the pristine Co_3O_4 in the sample and the Co_3O_4 generated from the oxidation of Co. The oxidation of Co increases the weight by 26.5%. Thus, taking 1 g sample for example, the following equation can be obtained:

$$m_{Co_3O_4} + 1.265 * m_{Co} = 0.586\ (g) \qquad (1)$$

where $m_{Co_3O_4}$ and m_{Co} are the mass (g) of Co_3O_4 and Co in 1 g sample.

In addition, the inductively coupled plasma (ICP) measurement was also performed to investigate the total mass of Co elements in sample. 1 g sample was dissolved by nitric acid for ICP measurement. The ICP result demonstrates that the total mass of Co element in sample is 0.461 g, which includes the mass of Co element in both Co and Co_3O_4. Considering that the mass ratio of Co element in Co_3O_4 is 73%, we can obtain the following equation:

$$0.73 * m_{Co_3O_4} + m_{Co} = 0.461\ (g) \qquad (2)$$

where $m_{Co_3O_4}$ and m_{Co} are the mass (g) of Co_3O_4 and Co in 1 g sample.

Consequently, based on equation (1) and (2), the mass of Co_3O_4 and Co in 1g sample is 0.438 and 0.032 g, respectively. Therefore, the percentage of Co_3O_4 and Co in the hybrid is 3.2% and 43.8%, respectively.

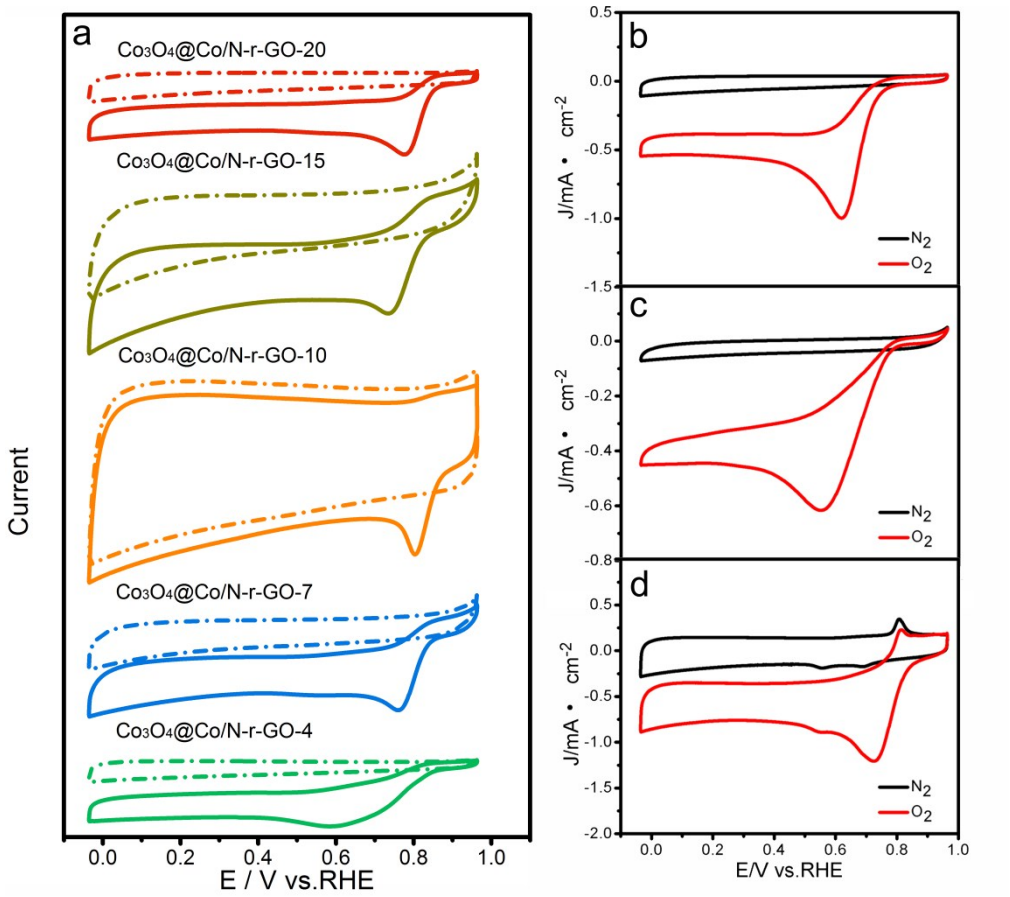

Figure S5. CV curves of Co_3O_4@Co/N-r-GO-x (a), Co_3O_4@Co/r-GO-10 (b), Co_3O_4@Co (c) and N-r-GO (d).

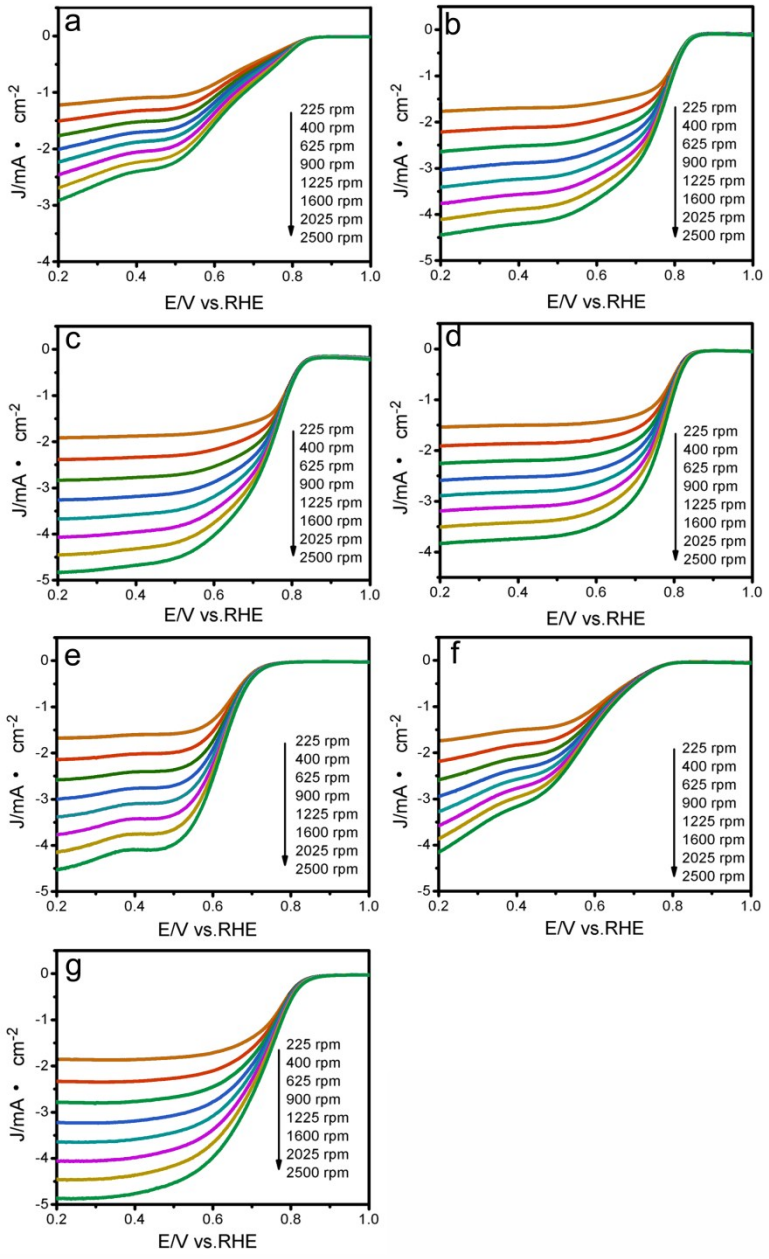

Figure S6. LSVs at different rotation speeds (from 225 to 2500 rpm) of Co_3O_4@Co/N-r-GO-4 (a), Co_3O_4@Co/N-r-GO-7 (b), Co_3O_4@Co/N-r-GO-15 (c), Co_3O_4@Co/N-r-GO-20 (d), Co_3O_4@Co/r-GO-10 (e), Co_3O_4@Co (f) and N-r-GO (g) and in 0.1 M KOH aqueous solution saturated with O_2.

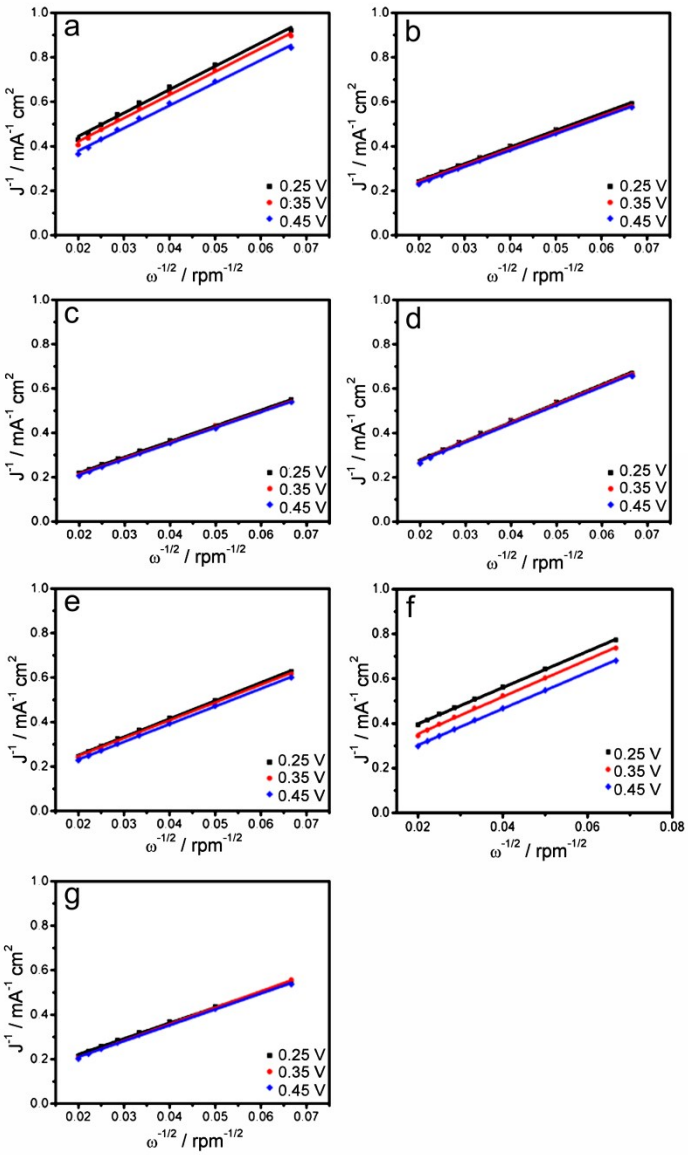

Figure S7. K-L plots at different potentials for RDE curves of Co_3O_4@Co/N-r-GO-4 (a), Co_3O_4@Co/N-r-GO-7 (b), Co_3O_4@Co/N-r-GO-15 (c), Co_3O_4@Co/N-r-GO-20 (d), Co_3O_4@Co/r-GO-10 (e), Co_3O_4@Co (f) and N-r-GO (g) in 0.1 M KOH aqueous solution saturated with O_2.

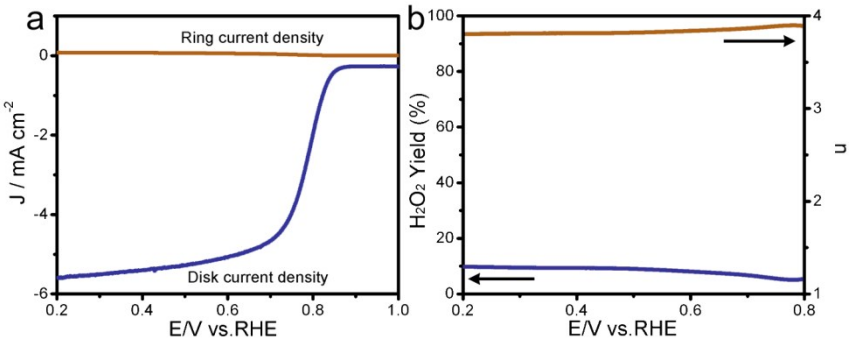

Figure S8. (a) LSVs curves of Co_3O_4@Co/N-r-GO-10 obtained by RRDE and (b) the corresponding H_2O_2 yield plots (blue line) and electron transfer number (brown line).

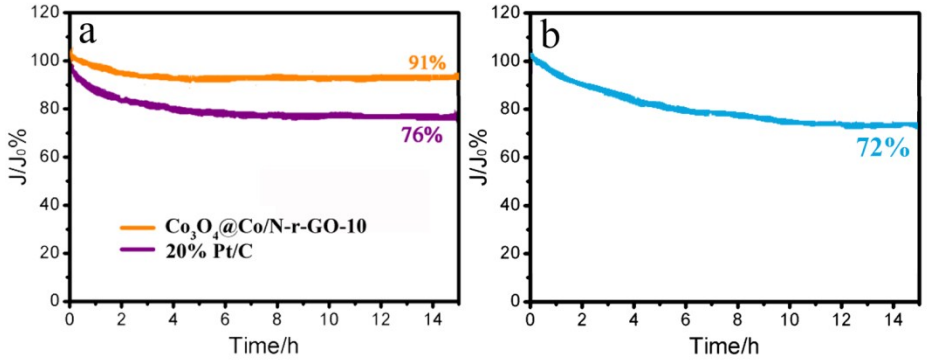

Figure S9. (a) Long-term stability test of Co_3O_4@Co/N-r-GO-10 in comparison with commercial 20% Pt/C for 15 h at 0.27 V in 0.1 M O_2-saturated KOH. (b) Long-term stability test of the sample without carbon layers for 15 h at 0.27 V in 0.1 M O_2-saturated KOH

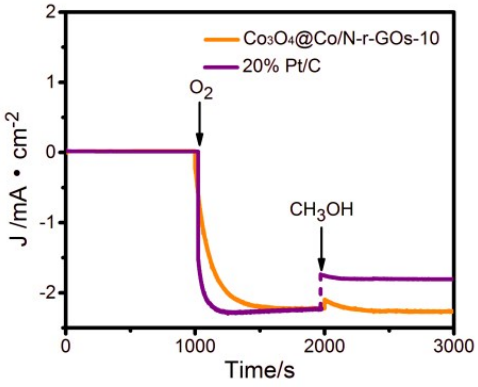

Figure S10. Methanol crossover resistance test of Co_3O_4@Co/N-r-GO-10 and 20% Pt/C at 0.7 V in 0.1 M KOH.

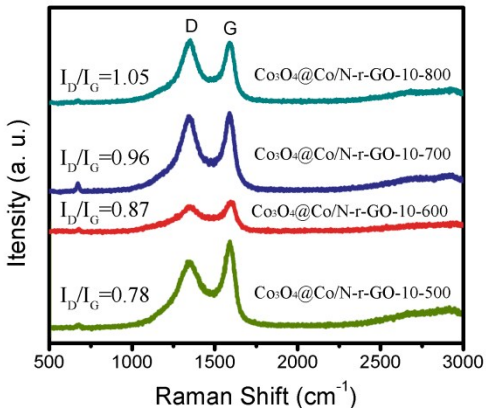

Figure S11. Raman spectroscopy of Co_3O_4@Co/N-r-GO-10-T (T = 500, 600, 700 and 800 °C).

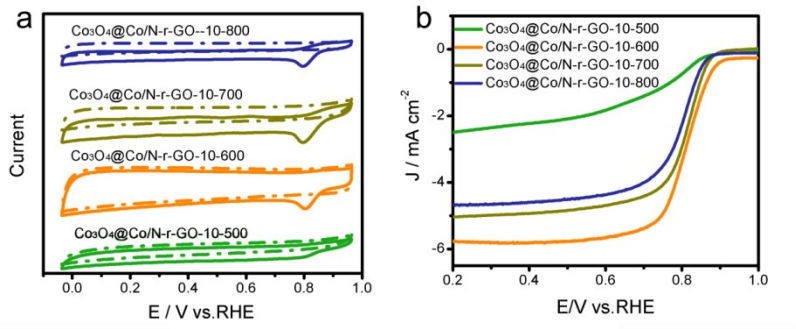

Figure S12. CV curves (a) and LSV curves at 1600 rpm (b) of Co_3O_4@Co/N-r-GO-10 pyrolyzed at different temperature (Co_3O_4@Co/N-r-GO-10-T, T=500, 600, 700, 800 °C).

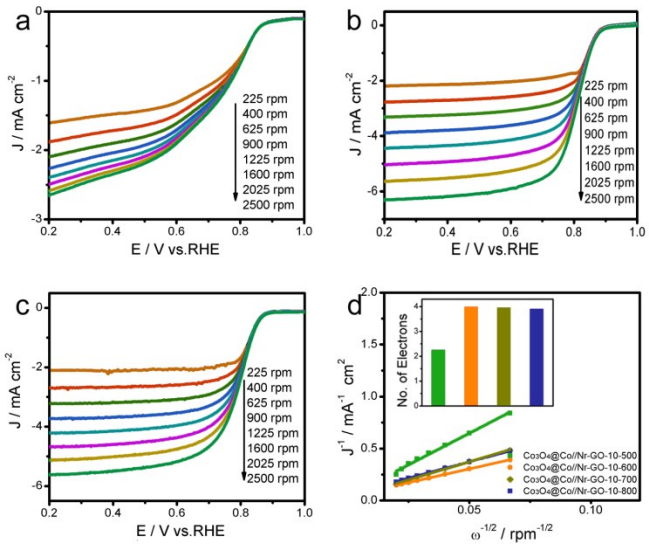

Figure S13. LSVs at different rotation speeds (from 225 to 2500 rpm) of Co_3O_4@Co/N-r-GO-10-500 (a), Co_3O_4@Co/N-r-GO-10-700 (b) and Co_3O_4@Co/N-r-GO-10-800 (c); (b) K-L plots for Co_3O_4@Co/N-r-GO-10-T obtained from LSVs at 0.35 V and the number of electrons respectively (inset).

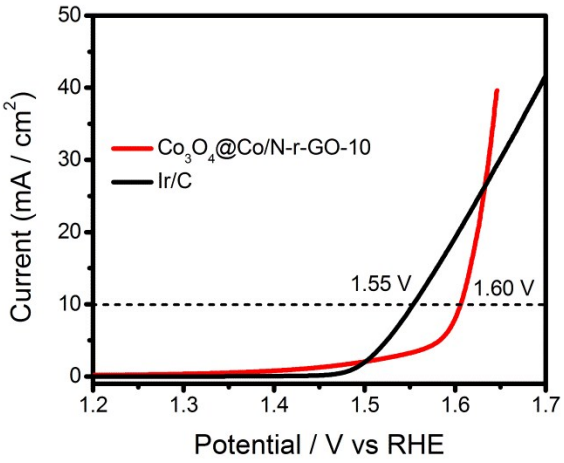

Figure S14. The OER activity of Co_3O_4@Co/N-r-GO-10 and commercial Ir/C.

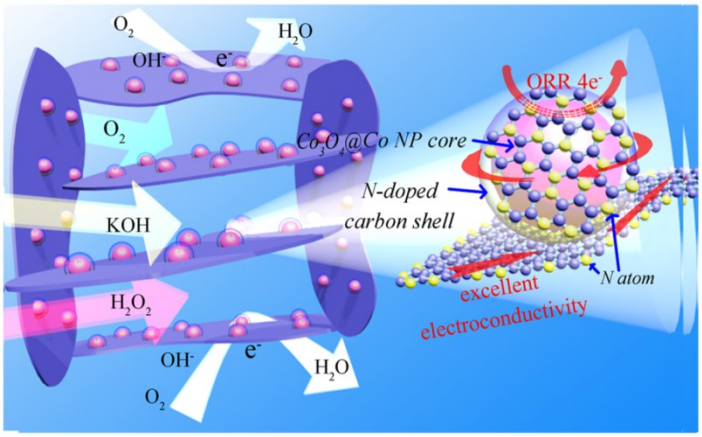

Figure S15. Illustration of the proposed reaction mechanism for ORR over the Co_3O_4@Co/N-r-GO-10

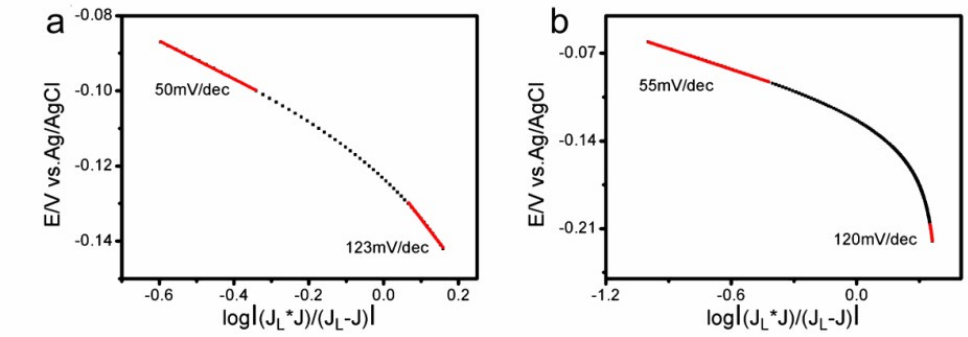

Figure S16. Linear fitting of Tafel plots at low and high over potentials regions for Co_3O_4@Co/N-r-GO-10 (a) and 20% Pt/C (b) in 0.1 M KOH aqueous solution saturated with O_2.

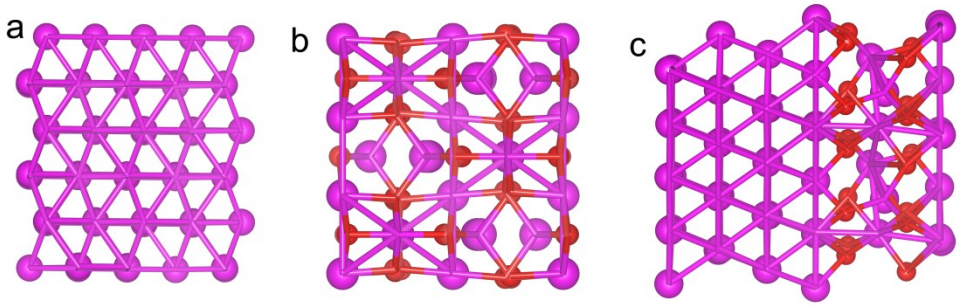

Figure S17. The optimized structural representations of Co (a), Co_3O_4 (b) and Co@Co_3O_4 (c).

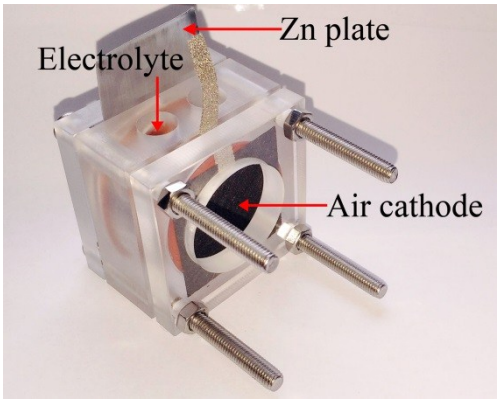

Figure S18. Digital image of the home-made ZABs.

Table S1. ORR performances of the samples obtained in this article.

Sample	E_{onset} **(V)**	$E_{1/2}$ **(V)**	$I_{limting}$ **(mA cm^{-2})**	***n* at 0.35 V**	J_k **(mA cm^{-2})**
20% Pt/C	0.98	0.81	−5.8	3.99	40
Co_3O_4@Co/N-r-GO-10	0.93	0.80	−5.4	3.98	38
Co_3O_4@Co/N-r-GO-4	0.87	0.62	−2.44	2.70	12
Co_3O_4@Co/N-r-GO-7	0.88	0.75	−3.8	3.82	15
Co_3O_4@Co/N-r-GO-15	0.89	0.74	−4.1	3.94	19
Co_3O_4@Co/N-r-GO-20	0.90	0.75	−3.2	3.33	14
N-r-GO	0.90	0.71	−4.1	3.81	25
Co_3O_4@Co	0.81	0.55	−3.1	3.34	15
Co_3O_4@Co/r-GO-10	0.80	0.61	−3.8	3.52	20

Table S2. A survey of primary ZABs with several key parameters extracted from the literature.

Reference	Catalysts	Loading (mg/cm^2)	Voltage	Durablity
This work	Co_3O_4@Co/N-r-GO-10	1.25	1.38 V @ 1 mA cm^{-2} 1.30 V @ 5 mA cm^{-2}	60 h @ 1 mA cm^{-2} 60 h @ 5 mA cm^{-2}
***Adv. Funct. Mater.* 2016, *26*, 4397-4404**	Co@NG-acid	1.08	1.30 V @ 10 mA cm^{-2} 1.20 V @ 50 mA cm^{-2}	14 h @ 10 mA cm^{-2} 4.5 h @ 50 mA cm^{-2}
***Angew. Chem. Int. Ed.* 2015, *54*, 9654-9658**	NCNT/CoO-NiO-NiCo	0.53	1.20 V @ 7 mA cm^{-2} 1.13 V @ 20 mA cm^{-2}	40000 s @ 7 mA cm^{-2} 30000 s @ 20 mA cm^{-2} 6000 s @ 35 mA cm^{-2}
***ACS Appl. Mater. Interfaces* 2015, 7, 21138-21149**	Co_3O_4/N-Doped Graphene	1	~ 1.25 V @ 10 mA cm^{-2}	> 30 h @ 10 mA cm^{-2}
***ACS Appl. Mater. Interfaces* 2015, 7, 17782-17791**	$Ag_{50}Cu_{50}$	Not mention	~ 1.13 V @ 20 mA cm^{-2}	40 h @ 20 mA cm^{-2}
***ACS Catal.* 2015, 5, 1445-1452**	CuPt-NC	2	~ 1.30 V @ 1 mA cm^{-2}	14 h @ 20 mA cm^{-2}
***Nat. Commun. 2013,4.*1805-1812**	CoO/N-CNT	1	~ 1.33 V @ 5 mA cm^{-2} ~ 1.2 V @ 20 mA cm^{-2}	22 h @ 5 mA cm^{-2} 12 h @ 50 mA cm^{-2}
***ACS Nano* 2015, 9, 6493-6501**	Carbon coated CuFe	Not mention	~ 1.1 V @ 100 mA cm^{-2} ~ 1.22 V @ 25 mA cm^{-2}	> 60 h @ 100 mA cm^{-2} > 60 h @ 25 mA cm^{-2}
***Adv. Energy Mater.* 2016, 1601052-1601058**	$Mn_xCo_{3-x}O_4$/ N-Ketjenblack	Not mention	~ 1.20 V @ 20 mA cm^{-2}	> 10 h @ 20 mA cm^{-2}
***J. Mater. Chem. A,* 2016, 4, 8602-8609**	N,P, Fe tri-doped porous carbon	Not mention	~ 1.38 V @ 1 mA cm^{-2} ~ 1.29 V @ 10 mA cm^{-2}	100 min @ 1 mA cm^{-2} 100 min @ 10 mA cm^{-2}

Reference

1. G. Kresse, J. Furthmüller, *Phys. Rev. B* **1996**, *54*, 11169.
2. G. Kresse, J. Furthmüller, *Computational Mater. Sci.* ***1996****, 6, 15.*
3. J. P. John, K. Burke, M. Ernzerhof, *Phys. Rev. Lett.* **1996**, *77*, 3865.